Effect of Spindle Speed and Feed Per Tooth in Feed Rate Perspective on Inconel HX Cutting Force

N. A. Mohd Nor, N. F. Kamarulzaman, N. A. S. Zakaria, N. Awang*
Department of Mechanical Engineering, School of Engineering,
Manipal International University, 71800 Putra Nilai, Malaysia.
** noraznan.namn@gmail.com*

B. T. H. T. Baharudin, M. K. A. Mohd Ariffin, Z. Leman
Department of Mechanical and Manufacturing Engineering,
Faculty of Engineering, Universiti Putra Malaysia,
43400 Serdang, Malaysia.

ABSTRACT

Reducing feed rate during end-milling of nickel-based superalloys for low-cutting force has always been a common approach. This is due to these alloys having superior properties, making them widely regarded as difficult-to-machine materials. As feed rate is tied to spindle speed and feed per tooth, it is crucial to comprehend whether spindle speed, feed per tooth or the interaction between spindle speed and feed per tooth has a significant factor on cutting force reduction when increasing the feed rate. Accordingly, this manuscript presents an effect of spindle speed and feed per tooth in feed rate perspective on Inconel HX cutting force. Half-immersion down-milling and full-immersion down-milling was conducted experimentally using solid ceramic end-mill cutter. The results indicate that cutting force decreases and then increases after further increase in spindle speed, while cutting force increases with an increase in feed per tooth. Optimum spindle speed and optimum feed per tooth for low-cutting force were 21,400 rpm and 0.013 mm/tooth. Furthermore, feed per tooth was the significant factor which influenced the cutting force, whereas spindle speed, and the interaction between spindle speed and feed per tooth were not significant.

Keywords: *Spindle speed; feed per tooth; down-milling; Inconel HX; cutting force*

ISSN 1823-5514, eISSN 2550-164X

Received for review: 2020-12-01
Accepted for publication: 2021-03-18
Published: 2021-04-15

Introduction

Cutting force or resultant force in end-milling is conveniently resolved into three cutting force components in the X, Y and Z axis. Firstly, the cutting force projection that acts along the feed direction or X-axis is defined as the feed force. Secondly, the cutting force projection in the Y-axis is called the normal force. Finally, the cutting force projection that acts in a perpendicular direction to the feed direction or Z-axis is called the axial force. On the other side, the findings from cutting force research have positively contributed to extending cutting tool life [1, 2], improved quality of machined material [2], reduction in production cost [3] and increase in production rate [4, 5]. Cutting force research findings are also key to curb carbon emissions due to climate change which is seen as top global threat. This is due to decrease in cutting force indirectly consumes less power for milling machine and can cause reduction in carbon emissions. As indicated by Hidayah et al. [6], approximately more than 70% of machining process is applied in the production sector in the world, and this sector has contributed about 36% of carbon emissions [7], thus reducing cutting force in end-milling can help in reducing the percentage of carbon emissions.

Apart from cutting force research findings, reducing feed rate and increasing cutting speed during end-milling of nickel-based superalloys have long been used for low-cutting force, as this difficult-to-machine material tends to be hard to end-mill [8, 9] which leads to high-cutting force due to its superior mechanical properties [8, 10]. The decrease in cutting force during reduction of feed rate is due to decrease in speed at which cutting tool engages the machined material [1]. Meanwhile, decrease in cutting force during increasing cutting speed is associated with increase in cutting temperature in the shear zone, and consequently softening the machined material due to drop in mechanical properties [11, 12]. In end-milling, feed rate is tied to spindle speed and feed per tooth, while cutting speed is tied to spindle speed. Decrease in feed per tooth indirectly decreases feed rate, and subsequently decreases cutting force. Whereas, increase in spindle speed not only increases cutting speed, but also increases feed rate. Therefore, a precise understanding whether spindle speed, feed per tooth or the interaction between spindle speed and feed per tooth is a significant factor on cutting force reduction when decreasing the feed rate is crucial.

In this manuscript, Inconel HX is selected as a specimen to study the effect of spindle speed and feed per tooth on cutting force in the feed rate perspective. It is one of the nickel-based superalloys and commonly used as a material for gas turbine engine applications [13] as it has high-strength at elevated temperatures [14] and outstanding oxidation resistance [15]. Besides, end-milling test performed experimentally by half-immersion down-milling and full-immersion down-milling as down-milling has been

recognised as the preferred method to end-mill difficult-to-machine materials compared to up-milling, since it reduces the load from the end-mill cutter edge, improves end-mill cutter life and leaves a better machined material surface quality. Solid ceramic end-mill cutter is used as it is an ideal solution to eliminate the role of cutting fluid due to its negative effect towards human health and environment [16], since this end-mill cutter has the ability to withstand high-cutting temperature during dry end-milling. The effect of spindle speed, feed per tooth and the interaction between spindle speed and feed per tooth are analysed systematically, therefore the optimum spindle speed and optimum feed per tooth for achieving low-cutting force is simultaneously proposed.

Experimental Setup

Experimental test for this research was carried out on a vertical machining centre model Mori Seiki NV 4000 DCG. Its maximum spindle speed is 30,000 rpm. The experimental set-up is illustrated in Table 1 where spindle speed and feed per tooth are divided into three levels. Since this research is focused on spindle speed and feed per tooth in feed rate perspective, there is no correlation between axial depth of cut and feed rate, thus axial depth of cut is held constant at 0.2 mm.

Table 1: Experimental setup

Cutting parameter	Level
Spindle speed (rpm)	16,000, 21,400 and 26,800
Feed per tooth (mm/tooth)	0.013, 0.016 and 0.019
Axial depth of cut (mm)	0.2

Dry end-milling of Inconel HX was performed by half-immersion down-milling and full-immersion down-milling using KYS40 solid ceramic end-mill diameter of 6 mm with 4 flutes from Kennametal. The dimension of Inconel HX specimen was 90 mm × 40 mm × 10 mm with original hardness 92 HR_B. Figure 1 and Figure 2 illustrate half-immersion down-milling and full-immersion down-milling performed in this experimental test. The cutting length was set at 22 mm per run. In addition, fresh KYS40 solid ceramic end-mill cutter was used at each run.

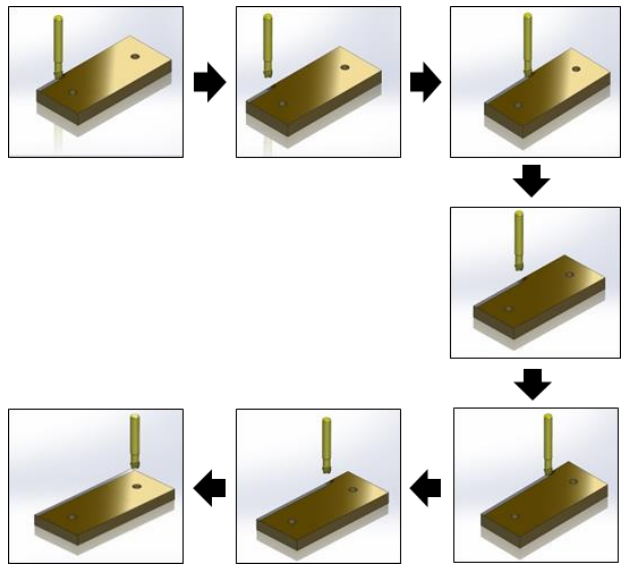

Figure 1: Half-immersion down-milling.

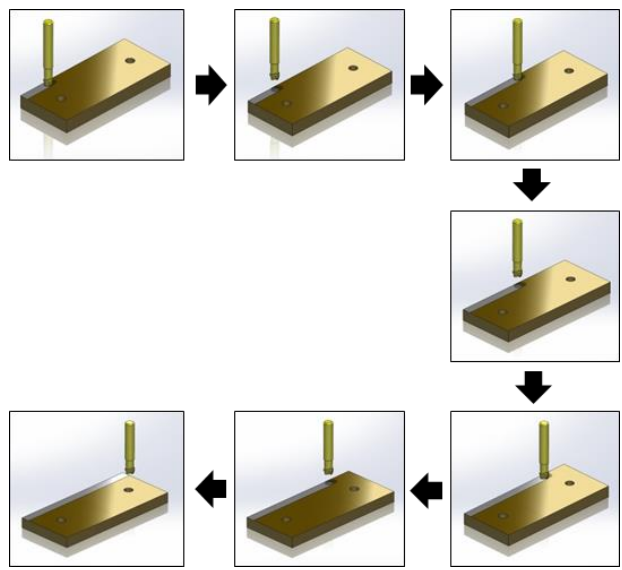

Figure 2: Full-immersion down-milling.

Cutting force components consisting of feed force (F_x), normal force (F_y), and axial force (F_z) were recorded using dynamometer type 9129AA from Kistler. The measurement was repeated three times at each run to find the average value. Figure 3 depicts the dynamometer measuring chain used in this experimental test.

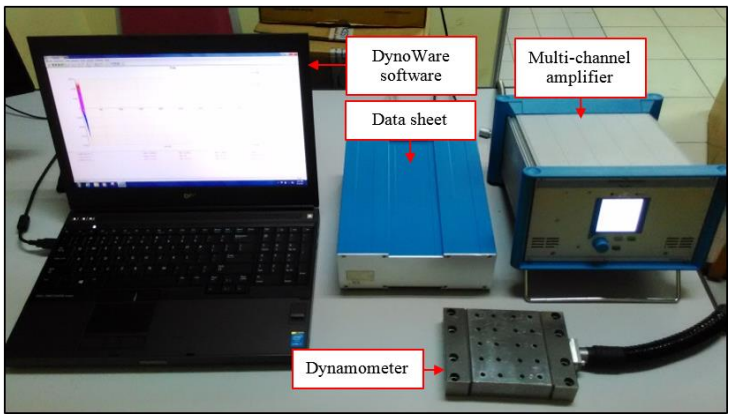

Figure 3: Dynamometer measuring chain.

The recorded cutting force components were then inserted into the Equation (1) [17] to compute the resultant force (F_r) or cutting force.

$$Fr = \sqrt{Fx^2 + Fy^2 + Fz^2} \quad (1)$$

From the computed cutting force, main effects plot and Pareto chart of the standardized effects in Minitab 19 were applied to perform analysis.

Results and Discussion

X-Y plots in Figure 4 and Figure 5 illustrate the overall results obtained after the recorded cutting force components were computed using Equation (1). X-axis and Y-axis represent spindle speed and cutting force respectively, while each trend-line represent feed per tooth at 0.013 mm/tooth (orange), 0.016 mm/tooth (lavender) and 0.019 mm/tooth (black). The effect of spindle speed and feed per tooth in feed rate perspective were discussed further based on the results obtained from main effects plot. Meanwhile, the factor that has significant effect on cutting force was discussed based on the results obtained from Pareto chart of the standardized effects.

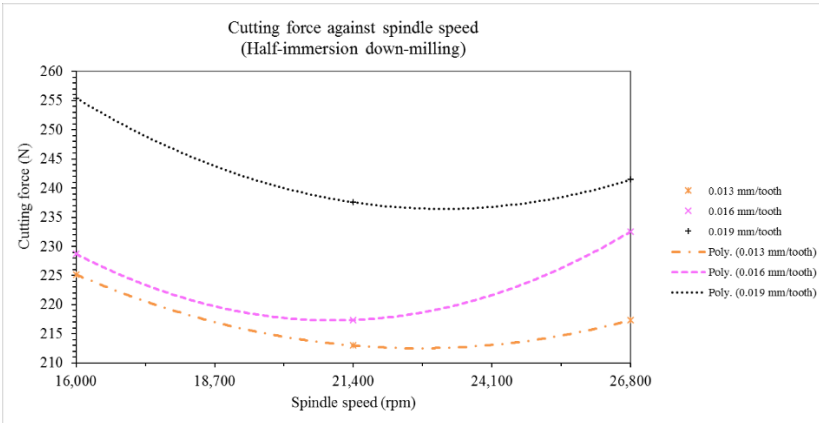

Figure 4: Cutting force against spindle speed for half-immersion down-milling.

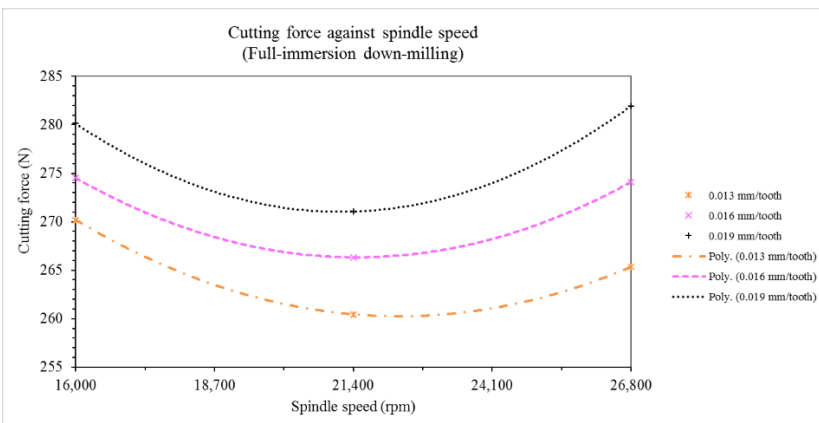

Figure 5: Cutting force against spindle speed for full-immersion down-milling.

Main effects in terms of mean cutting force (N) values for half-immersion down-milling and full-immersion down-milling were plotted in Figure 6 and Figure 7. It is evident from both plots that cutting force decrease when spindle speed increases from 16,000 rpm to 21,400 rpm, then start to increase when spindle speed increases higher from 21,400 to 26,800 rpm. This is contrary to [11, 18], which stated that the reduction of cutting

force is directly proportional to the increase in spindle speed. Furthermore, from both plots, it appears that spindle speed 21,400 rpm in half-immersion down-milling and full-immersion down-milling produced the lowest mean of cutting force, thus it can be claimed that increase in immersion amount or radial depth of cut does not influence the mean of cutting force. Following this, spindle speed 21,400 rpm can be classified as a critical spindle speed for both immersions due to the mean of cutting force drastically decrease before reaching 21,400 rpm and then increase again beyond this critical spindle speed. This can be related to the transition of machined material from ductile regime to brittle regime due to high-strain rate of the increased in spindle speed [19, 20]. In this scenario, Inconel HX undergoes brittle regime end-milling instead of ductile regime end-milling at spindle speed 21,400 rpm, whereby the chips of this end-milled material is removed due to brittle fracture that occurs at the point of tool-chip interface, and subsequently results in low mean of cutting force [21]. As expected, the mean of cutting force increases as the feed per tooth increases in both immersions. The observed increase in the mean of cutting force with increasing feed per tooth from 0.013 mm/tooth to 0.019 mm/tooth can be attributed to the probable increase in a shear amount of unwanted material at the end-mill cutter edge [1, 22]. Apart from this, feed per tooth 0.013 mm/tooth in both immersions are associated with the lowest mean of cutting force. From Figure 6 and Figure 7, it is observed that the optimum cutting parameters in achieving low cutting force are found to be at spindle speed 21,400 rpm and feed per tooth 0.013 mm/tooth, while the cutting force recorded were 213 N for half-immersion down-milling and 260 N for full-immersion down-milling.

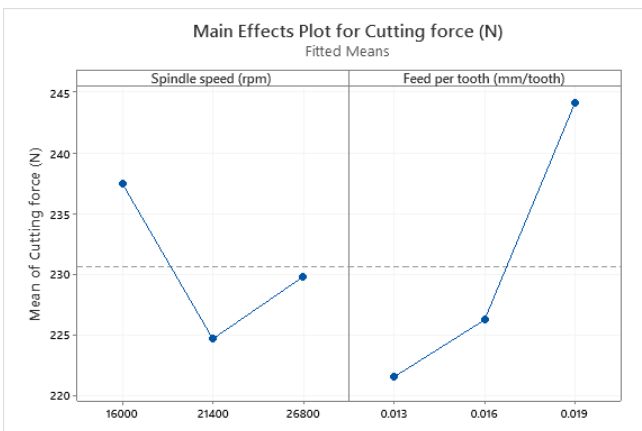

Figure 6: Main effects in terms of mean of cutting force (N) values for half-immersion down-milling.

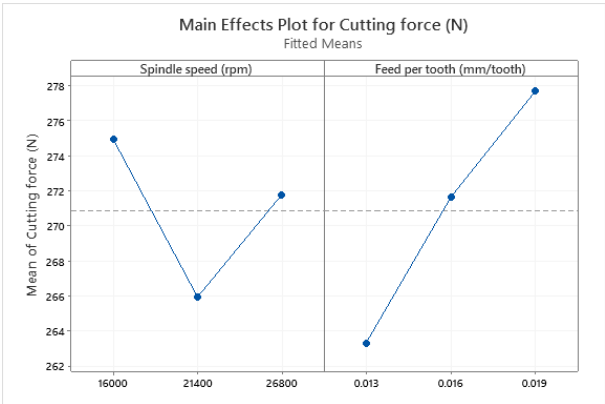

Figure 7: Main effects in terms of mean of cutting force (N) values for full-immersion down-milling.

Pareto chart of the standardized effects on cutting force were plotted in Figure 8 and Figure 9. The results show that B factor has the highest magnitude in half-immersion down-milling followed by A factor and AB factor. While in full-immersion down-milling, B Factor had the highest magnitude followed by AB factor and A factor. Furthermore, the reference line for both immersions was 2.571, therefore any factor that extended past this line was considered significant. It can be seen from Figure 8 and Figure 9 that feed per tooth is the significant factor in half-immersion down-milling and full-immersion down-milling. This is due to the increase in feed per tooth, whereas the mean of cutting force in both immersions also increases, as depict in Figure 6 and Figure 7. Meanwhile, spindle speed and the interaction between spindle speed and feed per tooth have effects on cutting force; however, both factors are not significant in half-immersion down-milling and full-immersion down-milling. In this scenario the mean of cutting force decreases and then increases after further increase in spindle speed, as can be seen in Figure 6 and Figure 7 this is the reason why spindle speed becomes insignificant factor on cutting force in both immersions. Since spindle speed has low magnitude and far from reference line as presented in Figure 8 and Figure 9, this scenario has led to interaction between spindle speed and feed per tooth to became insignificant factor on cutting force in half-immersion down-milling and full-immersion down-milling; although feed per tooth is the significant factor affecting cutting force in both immersions.

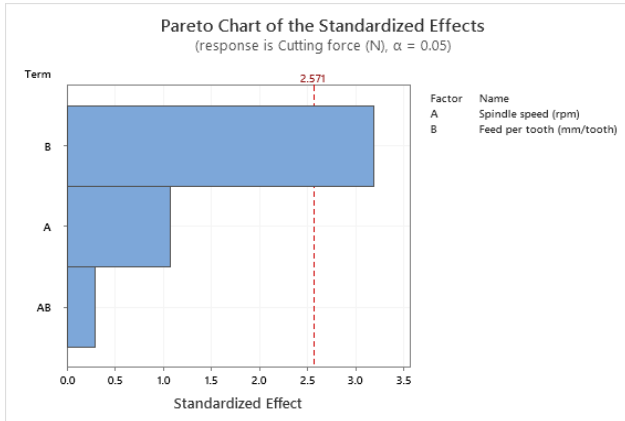

Figure 8: Pareto chart of the standardized effects on cutting force for half-immersion down-milling.

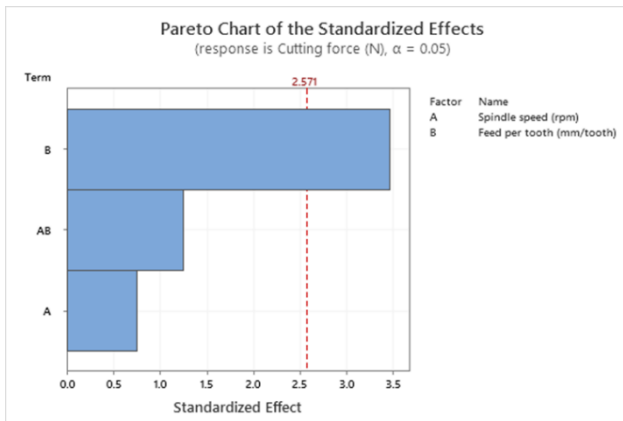

Figure 9: Pareto chart of the standardized effects on cutting force for full-immersion down-milling.

Finally, although spindle speed on cutting force is not a significant factor in feed rate perspective, spindle speed 21,400 rpm is enough to promote low-carbon manufacturing practices. This is due to spindle speed 21,400 rpm not being relatively high when considering Inconel HX as a machined material. Hence, low power consumption of machine tools can be obtained, and subsequently will curb carbon emissions [7]. In addition,

production sectors can reduce production cost due to low power consumption by using this spindle speed during end-milling of Inconel HX. Therefore, increasing spindle speed higher than 21,400 rpm or to its highest level for low-cutting force [11, 18], becomes unnecessary. Although Inconel HX had once been considered impractical to machine under dry condition, the use of KYS40 solid ceramic end-mill cutter in this experimental test proves that dry end-milling is practicable. Harmful effects of cutting fluid are becoming more apparent, mainly on human well-being and environment [23, 24]. Considering this issue, dry end-milling of Inconel HX using KYS40 solid ceramic end-mill cutter is the key for sustainable development.

Conclusion

In present research, the effects of spindle speed and feed per tooth in feed rate perspective on Inconel HX cutting force are studied. The following conclusions can be drawn from this research:

- Cutting force decreased when spindle speed is increased between 16,000 rpm and 21,400 rpm, and increased when using a spindle speed higher than 21,400 rpm.
- Cutting force increased with the increasing in feed per tooth.
- Spindle speed 21,400 rpm and feed per tooth 0.013 mm/tooth were an optimum cutting parameters as it was found to achieve low-cutting force.
- Feed per tooth was the significant factor affecting cutting force. Likewise, the effect of the spindle speed and the interaction between spindle speed and feed per tooth were not statistically significant.
- Future work should be focused on tool life and economical aspect of KYS40 solid ceramic end-mill cutter.

Acknowledgements

The results presented in this manuscript are part of the research project GP-IPS/2017/9539900 financed by Universiti Putra Malaysia. The authors would like to acknowledge Mr. Mohd Nor Bin Puteh, Mdm. Hatijah Binti Kassim, Mdm. Dyg. Siti Quraisyah Bt. Abg. Adenan and Mr. Nor Iman Ziqri Bin Nor Aznan for their support and encouragement.

References

[1] G. Bolar, A. Das, and S. N. Joshi, “Measurement and analysis of cutting

force and product surface quality during end-milling of thin-wall components," *Meas. J. Int. Meas. Confed.*, vol. 121, no. November 2017, pp. 190–204, 2018.
[2] J. Ma, D. Song, Z. Jia, G. Hu, W. Su, and L. Si, "Tool-path planning with constraint of cutting force fluctuation for curved surface machining," *Precis. Eng.*, vol. 51, pp. 614–624, 2018.
[3] Z. Xie, Y. Lu, and J. Li, "Development and testing of an integrated smart tool holder for four-component cutting force measurement," *Mech. Syst. Signal Process.*, vol. 93, pp. 225–240, 2017.
[4] M. Wan, W. Yin, and W.-H. Zhang, "Study on the Correction of cutting force measurement with table dynamometer," *Procedia CIRP*, vol. 56, pp. 119–123, 2016.
[5] M. Wan, W. Yin, W.-H. Zhang, and H. Liu, "Improved inverse filter for the correction of distorted measured cutting forces," *Int. J. Mech. Sci.*, vol. 120, pp. 276–285, 2017.
[6] M. T. Hidayah, J. A. Ghani, M. Z. Nuawi, and C. H. C. Haron, "A review of utilisation of cutting force analysis in cutting tool condition monitoring," *Int. J. Eng. Technol. IJET-IJENS*, vol. 15, no. 28, pp. 150203–4848, 2015.
[7] C. Tian, G. Zhou, J. Zhang, and C. Zhang, "Optimization of cutting parameters considering tool wear conditions in low-carbon manufacturing environment," *J. Clean. Prod.*, vol. 226, pp. 706–719, 2019.
[8] A. Pleta and L. Mears, "Cutting Force Investigation of Trochoidal milling in Nickel-based superalloy," *Procedia Manuf.*, vol. 5, pp. 1348–1356, 2016.
[9] D. Grguraš, M. Kern, and F. Pušavec, "Suitability of the full body ceramic end milling tools for high speed machining of nickel based alloy Inconel 718," *Procedia CIRP*, vol. 77, no. Hpc, pp. 630–633, 2018.
[10] D. Finkeldei, M. Sexauer, and F. Bleicher, "End milling of inconel 718 using solid Si3N4 ceramic cutting tools," *Procedia CIRP*, vol. 81, pp. 1131–1135, 2019.
[11] N. Masmiati, A. A. D. Sarhan, M. A. N. Hassan, and M. Hamdi, "Optimization of cutting conditions for minimum residual stress, cutting force and surface roughness in end milling of S50C medium carbon steel," *Meas. J. Int. Meas. Confed.*, vol. 86, pp. 253–265, 2016.
[12] H. Çalışkan and M. Küçükköse, "The effect of aCN/TiAlN coating on tool wear, cutting force, surface finish and chip morphology in face milling of Ti6Al4V superalloy," *Int. J. Refract. Met. Hard Mater.*, vol. 50, pp. 304–312, 2015.
[13] Q. Han, Y. Gu, S. Soe, F. Lacan, and R. Setchi, "Effect of hot cracking on the mechanical properties of Hastelloy X superalloy fabricated by laser powder bed fusion additive manufacturing," *Opt. Laser Technol.*,

vol. 124, p. 105984, 2020.
[14] A. R. K. Chennamsetty, J. Leblanc, S. Abotula, P. N. Parrikar, and A. Shukla, "Dynamic response of Hastelloy® X plates under oblique shocks: Experimental and numerical studies," *Int. J. Impact Eng.*, vol. 92, pp. 75–88, 2016.
[15] M. Esmaeilzadeh, F. Qods, H. Arabi, and B. M. Sadeghi, "An investigation on crack growth rate of fatigue and induction heating thermo-mechanical fatigue (TMF) in Hastelloy X superalloy via LEFM, EPFM and integration models," *Int. J. Fatigue*, vol. 97, pp. 135–149, 2017.
[16] A. Iturbe, E. Hormaetxe, A. Garay, and P. J. Arrazola, "Surface integrity analysis when machining Inconel 718 with conventional and cryogenic cooling," *Procedia CIRP*, vol. 45, no. Table 1, pp. 67–70, 2016.
[17] W. Shixiong, M. Wei, L. Bin, and W. Chengyong, "Trochoidal machining for the high-speed milling of pockets," *J. Mater. Process. Technol.*, vol. 233, pp. 29–43, 2016.
[18] A. Mebrahitom, W. Choon, and A. Azhari, "Side milling machining simulation using finite element analysis: *Prediction of Cutting Forces*," Mater. Today Proc., vol. 4, no. 4, Part D, pp. 5215–5221, 2017.
[19] B. Wang, Z. Liu, G. Su, Q. Song, and X. Ai, "Investigations of critical cutting speed and ductile-to-brittle transition mechanism for workpiece material in ultra-high speed machining," *Int. J. Mech. Sci.*, vol. 104, pp. 44–59, 2015.
[20] N. A. Mohd Nor, B. T. H. T. Baharudin, J. A. Ghani, Z. Leman, and M. K. A. Mohd Ariffin, "Effect of chip load and spindle speed on cutting force of Hastelloy X," *J. Mech. Eng. Sci.*, vol. 14, no. 1, pp. 6497–6503, 2020.
[21] B. Wang, Z. Liu, G. Su, and X. Ai, "Brittle removal mechanism of ductile materials with Ultrahigh-speed machining," *J. Manuf. Sci. Eng. Trans. ASME*, vol. 137, no. 6, 2015.
[22] V. Gaikhe, J. Sahu, and R. Pawade, "Optimization of cutting parameters for cutting force minimization in helical ball end milling of inconel 718 by using genetic algorithm," *Procedia CIRP*, vol. 77, no. Hpc, pp. 477–480, 2018.
[23] N.A. Mohd Nor, S.S. Mohd Alisjabana, G. Seloraji, Y. M. Tee, J. X. Teh, B.T.H.T. Baharudin, M.K.A. Mohd Ariffin, and Z. Leman, "Effect and optimization of cutting speed and depth of cut in half-immersion up-milling of 6061 aluminium alloy," *J. Mech. Eng.*, vol. 16, no. 1, pp. 17–27, 2019.
[24] N. A. Mohd Nor, B. T. H. T. Baharudin, M. K. A. Mohd Ariffin, and Z. Leman, "Effect of compressed air and cutting speed on surface roughness of 6061 aluminium alloy," *J. Mech. Eng.*, vol. 16, no. 2, pp. 53–62, 2019.